

# Numerical Analysis of the Effect of Geocell Reinforcement above Buried Pipes on Surface Settlement and Vertical Pressure

Waqed H. Almohammed, Mohammed Y. Fattah, Sajjad E. Rasheed

**Abstract**—Dynamic traffic loads cause deformation of underground pipes, resulting in vehicle discomfort. This makes it necessary to reinforce the layers of soil above underground pipes. In this study, the subbase layer was reinforced. Finite element software (PLAXIS 3D) was used in the simulation, which includes geocell reinforcement, vehicle loading, soil layers and Glass Fiber Reinforced Plastic (GRP) pipe. Geocell reinforcement was modeled using a geogrid element, which was defined as a slender structure element that has the ability to withstand axial stresses but not to resist bending. Geogrids cannot withstand compression but they can withstand tensile forces. Comparisons have been made between the numerical models and experimental works, and a good agreement was obtained. Using the mathematical model, the performance of three different pipes of diameter 600 mm, 800 mm, and 1000 mm, and three different vehicular speeds of 20 km/h, 40 km/h, and 60 km/h, was examined to determine their impact on surface settlement and vertical pressure at the pipe crown for two cases: with and without geocell reinforcement. The results showed that, for a pipe diameter of 600 mm under geocell reinforcement, surface settlement decreases by 94 % when the speed of the vehicle is 20 km/h and by 98% when the speed of the vehicle is 60 km/h. Vertical pressure decreases by 81 % when the diameter of the pipe is 600 mm, while the value decreases to 58 % for a pipe with diameter 1000 mm. The results show that geocell reinforcement causes a significant and positive reduction in surface settlement and vertical stress above the pipe crown, leading to an increase in pipe safety.

**Keywords**—Dynamic loading, geocell reinforcement, GRP pipe, PLAXIS 3D, surface settlement.

## I. INTRODUCTION

**B**URIED pipes play an important role in city infrastructure. However, they must support the weight of the surrounding soil, and therefore, they must be protected and properly installed to avoid serious ramifications to the pipe system, the above pavement, and the buildings. Buried pipes and/or conduits have improved the standard of living for people since the beginning of civilization. Furthermore, engineers and planners take subsurface infrastructure into account before developing buildings and houses for a community. In addition, the underground water systems can

be seen as the city's arteries and the sewer systems are the city's veins that carry the waste [1].

Generally, reinforcing the subbase layer will increase its stiffness and, therefore, reduce the surface settlement. A number of researchers have used numerical simulation on the buried pipes problem. Geocells are commonly used geosynthetic reinforcements, they can provide lateral constraint to the granular materials. The geocells are placed at grade, in-filled with well grade soil, and they are then compacted. The cellular structures of the geocells improve the vertical and lateral confinement, and tensioned membrane effect, which leads to an increase in the bearing capacity and an increase in the stress distribution [2]. So, permanent deformations or rutting beneath the traffic loading can be reduced. Typically, the geocell-base/subbase framework is underlain by a geotextile to separate the in-filled base/subbase material from the subgrade. Reference [3] carried out laboratory tests and numerical simulation on the use of geocell reinforcement with rubber mixture to protect underground pipes under repeated loading. Their results showed that reinforcement can reduce surface settlement for different conditions. Reference [4] used the finite element software PLAXIS 2D to analyze the performance of unreinforced and geogrid reinforced pavement under static and dynamic loads. Their results showed that the reinforced layers have a moderate improvement over the unreinforced layer under static load but no improvement was shown under dynamic load. Their results also showed that adding another geogrid layer led to no significant improvement. Reference [5] dealt with simulation of the buried pipe problem numerically by finite elements method using the newest version of PLAXIS-3D software. A three-dimensional analysis was made by PLAXIS-3D program for [6], which has all the properties needed, such as the modulus of elasticity, Poisson's ratio, and angle of internal friction. Results obtained from the program for the vertical crown deflection for the model without geogrid are higher than those obtained by two-dimensional plane strain by about 21.4%, while with geogrid, results showed that this percent becomes 12.1% although generally both have the same trend. Predictions of pipe-soil system behavior with applied pressure obtained from the two-dimensional finite element's analysis indicate an almost linear displacement of pipe deflection; while a non-linear behavior, especially at higher loads, was found from the three-dimensional analysis.

Reference [7] conducted laboratory experiments on a flexible Poly Vinyl Chloride (PVC) pipe with a small diameter

Waqed H. Al Muhammed is Assistance Professor at the Department of Civil Engineering, University of Kerbala, Kerbala, Iraq (phone: +9647801146150; email: Waaqidh@uokerbala.edu.iq, waqed2005@yahoo.com).

Mohammed Y. Fattah is Professor at Building and Constriction Engineering Dep., University of Technology, Baghdad, Iraq.

Sajjad E. Rasheed is Graduate student from Civil Engineering Department, University of Kerbala, Kerbala, Iraq.

that was buried in sand beds reinforced with geocells. This experiment aimed to investigate the use of geocell reinforcement in protecting buried pipe systems, and to protect underground utilities and structures from vehicle loadings. The selected pipe had a thickness of 1.4 mm and an outside diameter of 110 mm. A dynamic repeated loading was applied to a steel plate above the sand surface to simulate vehicle loading. A number of laboratory tests have been conducted to study the behavior of geocell-reinforced sand that was subjected to dynamic loading. These results showed that the optimum depth of geocell reinforcement was 0.1 of the steel footing width and the optimum width of the geocell reinforcement was 3.2 times the width of the steel footing ( $u/B = 0.1$  and  $b/B = 3.2$ ).

This paper deals with the numerical simulation of the effect of geocell reinforcement on the surface settlement and vertical stress above buried pipes.

## II. FINITE ELEMENT ANALYSIS

The static formulation of the employed finite element method in PLAXIS 3D is briefly presented here, the equation of time-dependent movement of a volume influenced by dynamic loading is [8]:

$$M \ddot{U} + C \dot{U} + K U = F \quad (1)$$

where:  $M$  is the mass matrix,  $\ddot{U}$  is the acceleration,  $C$  is the damping matrix,  $\dot{U}$  is the velocity,  $K$  is the stiffness matrix,  $U$  is the displacement vector, and  $F$  is the load vector.

The two terms in (1) ( $K U = F$ ) are related to the static deformation. In the matrix  $M$ , the materials' mass (water, soil and any constructions) is considered. In PLAXIS 3D, the mass matrix is executed as a lumped matrix. The damping of the materials is presented by matrix  $C$ . In reality, irreversible deformations (plasticity or viscosity) or friction cause material damping. More vibration energy can be dissipated with either more plasticity or more viscosity. The phenomena of damping can still be considered using matrix  $C$  if elasticity is assumed. In the finite element formulations,  $C$  is often expressed as a function of the mass and stiffness matrices (Rayleigh damping) [9] as:

$$C = \alpha R M + \beta R K \quad (2)$$

where  $\alpha R$  is the mass proportional Rayleigh damping coefficient and  $\beta R$  is the stiffness proportional Rayleigh damping coefficient. The soil elements in 3D finite element mesh are modeled as tetrahedral elements with 10 nodes, as shown in Fig. 1. Soil has a tendency to behave in a non-linear manner under load. This non-linear stress-strain conduct may be modeled at a few levels of modernity. Obviously, the number of parameters in the model expands with the level for refinement. PLAXIS 3D can support a number of models to simulate soil behavior. Due to the lack of knowledge and available testing equipment, the Mohr-Coulomb model (MC) is used to simulate the sand and subbase layers. The MC model (linear elastic perfectly plastic) failure contour requires

five input parameters, which are familiar to most civil engineers and can be calculated from basic soil tests. The five parameters of the MC model (in case of the drain behavior) are:  $E'$ , which is effective modulus of Young ( $\text{kN/m}^2$ ); and  $\nu'$ , which is Poisson's ratio. The other MC parameters are:  $\phi'$ , which is the effective friction angle;  $c'_{\text{ref}}$ , which is effective cohesion, ( $\text{kN/m}^2$ ); and  $\psi$ , which is the dilatancy angle.

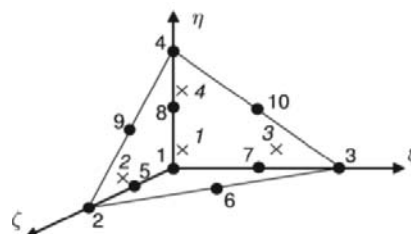


Fig. 1 Three-dimensional soil elements (10-node tetrahedrons)

Special measures are needed at the boundaries to counter the reflections, especially for viscous boundaries. Various methods can be used to create these boundaries, which include:

- Half-infinite elements (boundary elements);
- Adaptation of the material properties of the elements at the boundary (low stiffness, high viscosity); and
- Viscous boundaries (dampers).

Default fixities were chosen in favor of the viscous boundaries because viscous boundaries move the boundary horizontally, and therefore, produce false results.

A total of 18 models will be simulated in this study. Nine of them are unreinforced and the other nine are reinforced. The following three different pipe diameters were selected: 600 mm, 800 mm, and 1000 mm. The depth of each pipe was set as a function to diameter ( $1.67D$ ) in order to provide the minimum cover required for smallest diameter used. The following three vehicle speeds were chosen: 20 km/h, 40 km/h, and 60 km/h. The geocell reinforcement was modeled at the sand-subbase interface. Fig. 2 presents a summary of the numerical analysis program that was conducted in the parametric study and Fig. 3 shows a cross-section of the model. Fig. 5 presents the mesh view of the model, showing the location of points for curve generation.

Figs. 5-7 show the traffic loading wave for all of the simulated vehicle speeds. Table I presents the properties of the soils, asphalt, GRP pipe and geocells materials that were used in the parametric study. Some of the parameters of the asphalt and subbase layers are assumed and the parameters of the GRP pipe are provided by the manufacturer. To calculate the soil pressure on the flexible pipe, the loading is normally assumed to be a HL-93 design truck. Design truck consists of three axles, one on the front with 8 kip (35 kN) weight and two on the rear with weight 32 kip (145 kN) of both. The front and rear axles' distance is 14 feet (4.3 m) and that distance between the rear axles is ranged from 14 feet (4.3 m) to 30 feet (9.0 m), which is designed to obtain the worst design force. Tires distance for each axle is 6 feet (1.8 m).

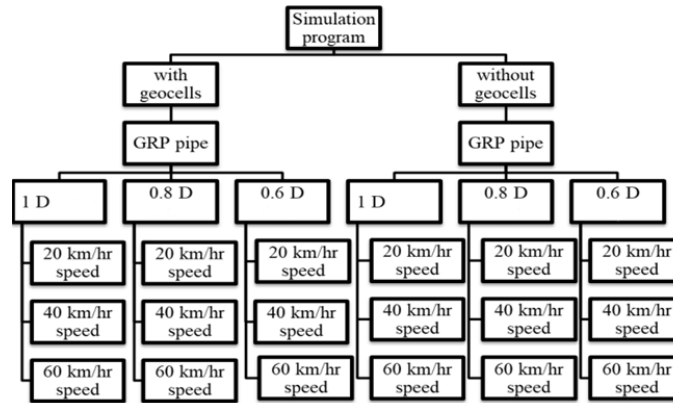


Fig. 2 Summary of the finite element analysis models

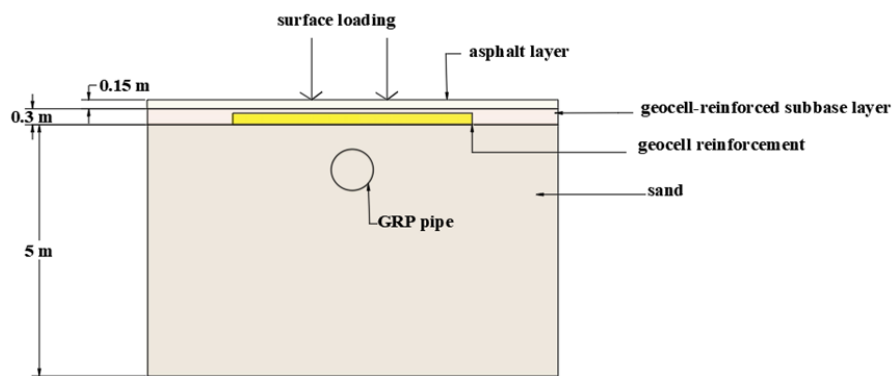


Fig. 3 Cross-section of the model

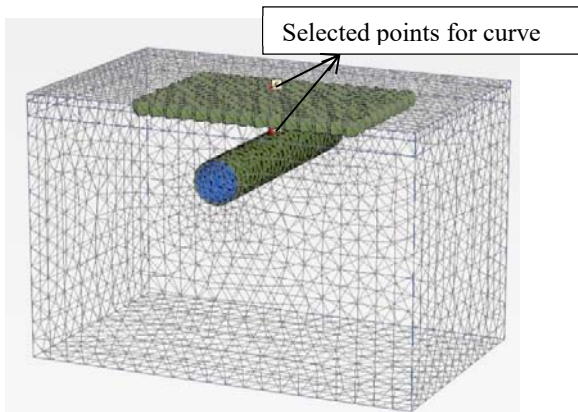


Fig. 4 Mesh view of the model, showing the location of points for curve generation

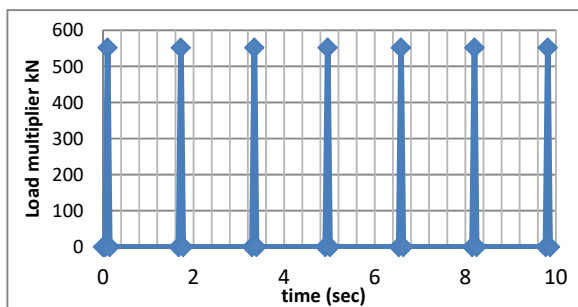


Fig. 5 Dynamic loading wave (speed = 20 km/h)

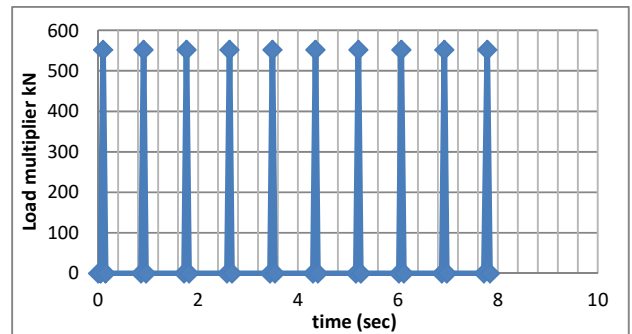


Fig. 6 Dynamic loading wave (speed = 40 km/h)

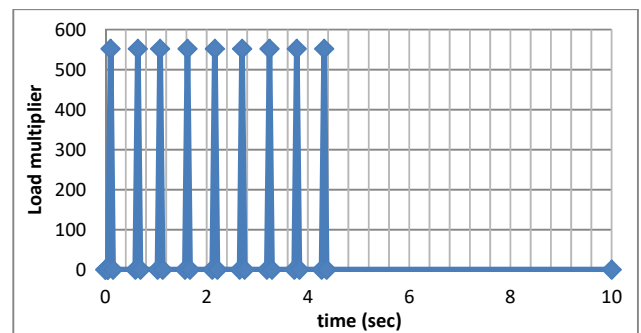


Fig. 7 Dynamic loading wave (speed = 60 km/h)

TABLE I  
 MATERIAL PROPERTIES

Soil	Sand	Subbase	Asphalt	GRP pipe
Model	Mohr-Coulomb	Mohr-Coulomb	Linear elastic	Plate element
Unit weight $\gamma$ (kN/m <sup>3</sup> )	17.2	22.06	23.5	15.8
Modulus of elasticity $E'$ (kN/m <sup>2</sup> )	35000	120000	12000000	41000000
Angle of friction $\Phi'$ (°)	38	40	-	-
Dilatancy angle $\psi$ (°)	8	10	-	-
Poisson's ratio	0.3	0.35	0.3	0.159

### III. MODEL VERIFICATION

The finite element model was calibrated based on the results of the experimental work conducted by [10]. The experimental work was conducted in a cubic steel box that was used for this experiment. The box has an 800 mm width, which agrees with the recommendations of [11], [12]. According to [11], the width of the trench should have a minimum value that is equal to or more than 1.25 times the outside diameter of the pipe with a 300-mm addition. Reference [12] also recommends that the width of the trench should be equal to or more than the pipe outside diameter 110 mm with an addition of 300 mm. The other two dimensions of the steel box were also made to be 800 mm, and they made up from 6 mm thick steel plates.

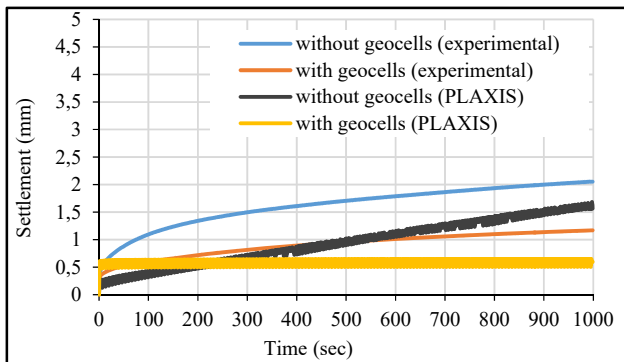


Fig. 8 Comparison between the experimental and the numerical simulation for surface settlement versus time ( $a = 0.5$  ton,  $\omega = 0.5$  Hz)

By using the geogrid element, which is defined as a slender structure element, the geocell reinforcement was modelled. The axial stresses can be overcome by the slender structure element, but the last cannot resist bending. Although geogrids have the capability to resist tensile forces; but, it cannot withstand in front of compression forces. This modeling was found to be successful through good convergence with experimental results. This study's results showed that numerical modeling can co-operate well with the experimental work results. The results show that the maximum difference between the experimental and the numerical results is about 1 mm, and the maximum difference between the experimental and the numerical results is about 1.5 kN/m<sup>2</sup> at the end of the dynamic test. The convergence of the results was achieved after numerous trails and changes to the input parameters in PLAXIS 3D software. Figs. 8 and 9 present the verification

results for the surface settlement and the vertical stress with frequency of the load ( $\omega=0.5$  Hz), load amplitude ( $a=0.5$  ton), respectively.

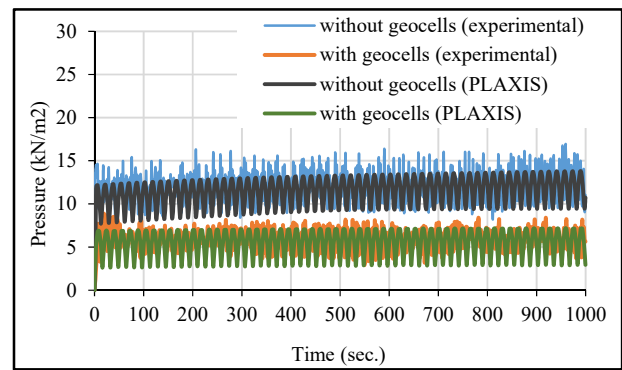


Fig. 9 Comparison between the experimental and the numerical simulation for vertical pressure versus time ( $a = 0.5$  ton,  $\omega = 0.5$  Hz)

### IV. RESULTS AND DISCUSSION

#### A. Surface Settlement

Figs. 10–13 present the results for surface settlement. When the pipe diameter is 600 mm with the geocell reinforcement, the surface settlement decreases by 94 % when the speed of the vehicle is 20 km/h, by 95% when the speed of the vehicle is 40 km/h and by 98% when the speed of the vehicle is 60 km/h. When the pipe diameter is 800 mm and when using the geocell reinforcement, the surface settlement decreases by almost the same values as those for the 600-mm diameter pipe and for all of the vehicle speeds. Increasing the pipe diameter to 1000 mm will lead to the same reduction in terms of surface settlement for all of the simulated speeds. So, it could be said that there is no effect in increasing the speed with a pipe diameter equal to 1000 mm. The similarity of the results may be attributed to the high values of stiffness for both the asphalt and the subbase layers, the large values of modulus of elasticity will lead to a small value of surface settlement 1.03 mm. When adding the geocell reinforcement, the surface settlement becomes much less 0.03 mm due to the increase of stiffness of reinforced subbase layer. Table II presents a summary of the surface settlement results.

Geogrids or geocells provide reinforcement by laterally restraining the base or subbase and improving the bearing capacity of the system, thus decreasing shear stresses on the weak subgrade. In addition, the confinement provided by geogrids improves the distribution of the vertical pressure above the subgrade and decreases subgrade vertical

deformation. The geogrid aperture size to aggregate grain size appropriate ratio is an important factor that affects the performance of geogrid reinforcement systems [13]. The infill materials' modulus and strength can be increased as it was stated by the previous studies (e.g. [14], [15]). However, large-scale testing of geocell-reinforced aggregates which are placed on poor soils has yet limited information to evaluate the field work of large pipes in regarding to the degree of improvement and performance, which are obtained and examined in this work. Furthermore, geocell mesh provides better interlocking with the soil particles, thus ensuring adequate anchorage during loading. The load carrying capacity enhancement could be credited to the load dispersion improvement through a reinforced subbase on to the subgrade. This leads to less stress intensity being transferred to the subgrade, which leads to less distress in the subgrade.

Fig. 14 shows a comparison of the surface settlement at the pipe crown both with and without geocell reinforcement, and for the same pipe diameters and loading. It is clear from these figures that surface settlement decreased significantly due to the presence of the geocell reinforcement within the subbase layer.

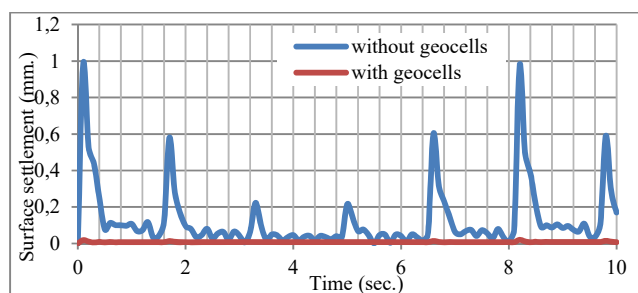


Fig. 10 Surface settlement versus time when (D=600 mm, S=20 km/h)

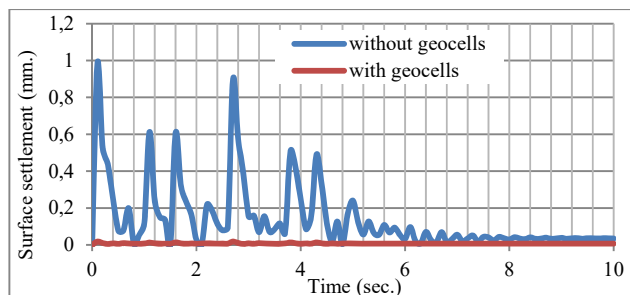


Fig. 11 Surface settlement versus time when (D=600 mm, S=60 km/h)

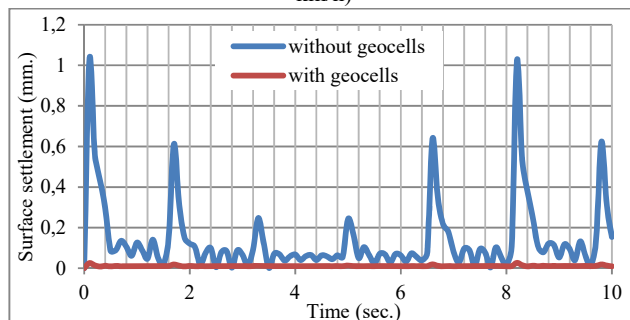


Fig. 12 Surface settlement versus time when (D=1000 mm, S=20 km/h)

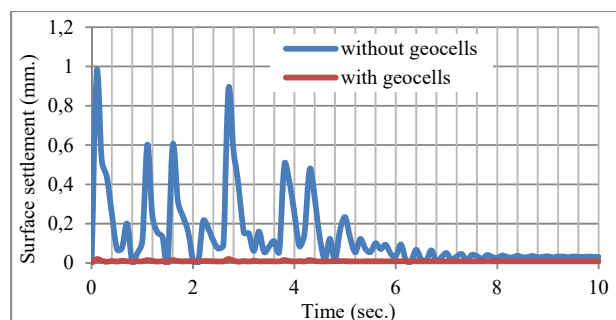


Fig. 13 Surface settlement versus time when (D=1000 mm, S=60 km/h)

TABLE II  
 SURFACE SETTLEMENT RESULTS

Pipe diameter (mm) Model	Surface settlement(mm)						Reduction percentage		
	Without geocells			With geocells			20 km/h	40 km/h	60 km/h
	20 km/h	40 km/h	60 km/h	20 km/h	40 km/h	60 km/h			
600	0.98	0.98	0.98	0.06	0.05	0.021	94 %	95 %	98 %
800	0.98	0.97	0.97	0.05	0.03	0.019	95 %	96 %	97 %
1000	1.03	1.03	0.98	0.03	0.03	0.02	97 %	97 %	98 %

### B. Vertical Pressure

Figs. 15–18 present the results for vertical stress at the pipe crown. When the pipe diameter is 600 mm and when using the geocell reinforcement, the vertical pressure decreases by 81% when the vehicle speed is 20 km/h, and by 82% when the vehicle speed is 40 km/h, and by 81% when the vehicle speed is 60 km/h. When the pipe diameter is 800 mm and when using the geocell reinforcement, the percentage becomes 75% for all values of vehicle speed (i.e. 20 km/h, 40 km/h, and 60 km/h). When the pipe diameter is increased to 1000 mm and

using the geocell reinforcement, the values of decrement become 59% when the vehicle speed is 20 km/h, 58% when the vehicle speed is 40 km/h, and 57% when the vehicle speed is 60 km/h. These results show that the vertical pressure decreases when the pipe diameter increases, while these values do not change significantly for different speeds for the same pipe diameter.

Table III presents a summary of the results of vertical pressure on pipes of diameters 600 mm, 800 mm, and 1000 mm and using three different speeds of 20 km/h, 40 km/h, and

60 km/h.

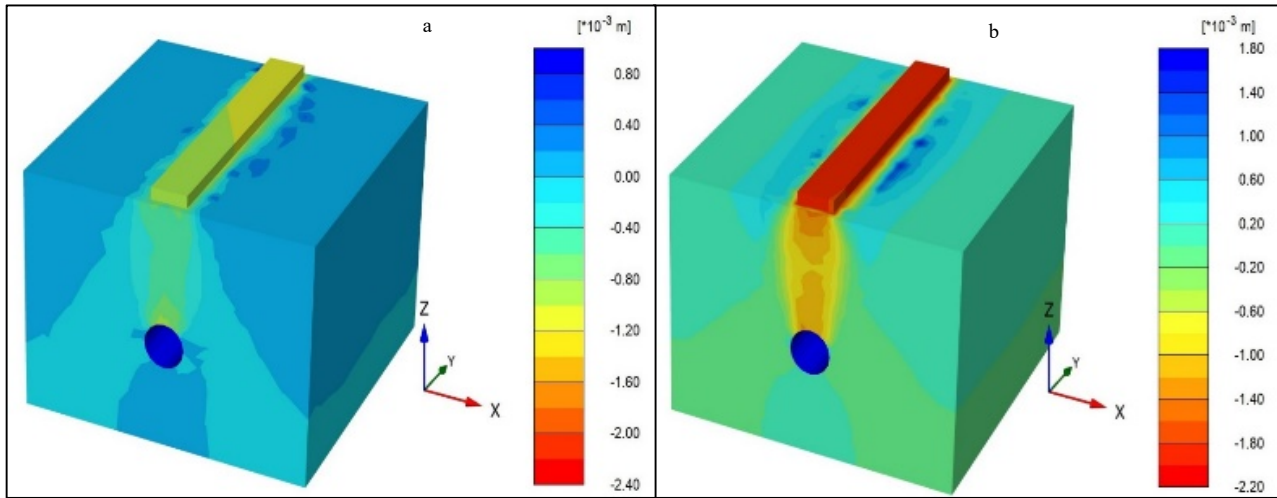


Fig. 14 Numerical surface settlement results for (a) reinforced (b) unreinforced

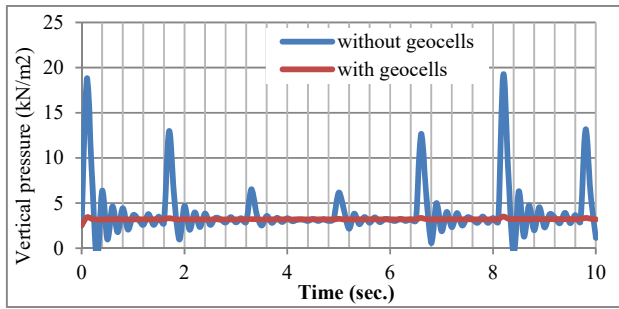


Fig. 15 Vertical pressure versus time when (D=600 mm, S=20 km/h)

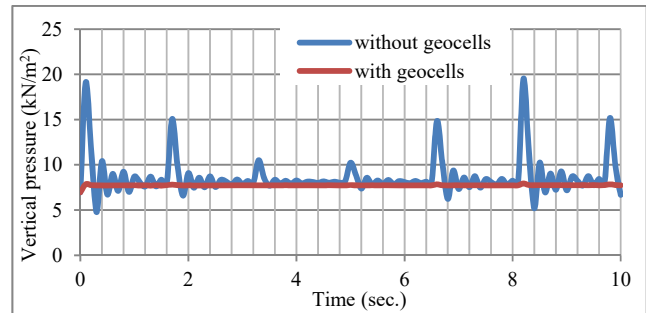


Fig. 17 Vertical pressure versus time when (D=1000 mm, S=20 km/h)

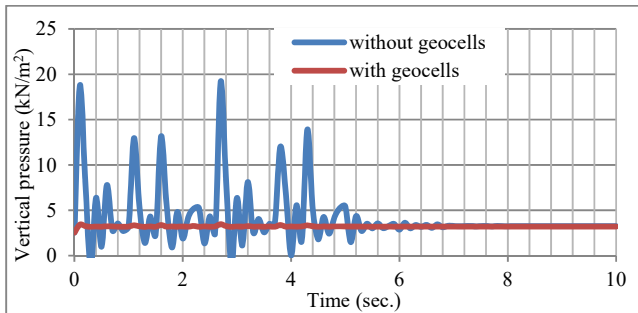


Fig. 16 Vertical pressure versus time when (D=600 mm, S=60 km/h)

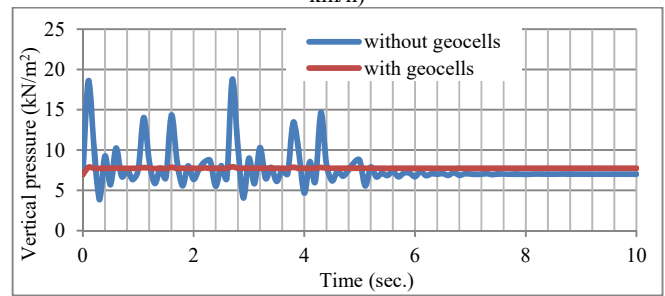


Fig. 18 Vertical pressure versus time when (D=1000 mm, S=60 km/h)

TABLE III  
 RESULTS OF VERTICAL PRESSURE AT THE PIPE CROWN

Pipe diameter (mm) Model	Vertical pressure(kN/m <sup>2</sup> )						Reduction percentage		
	Without geocells			With geocells			20 km/h	40 km/h	60 km/h
	20 km/h	40 km/h	60 km/h	20 km/h	40 km/h	60 km/h			
600	19.23	18.76	19.18	3.5	3.43	3.46	81 %	81 %	82 %
800	16.45	16.25	16.47	4	3.98	4	75 %	75 %	75 %
1000	19.51	19.09	18.75	7.9	7.89	7.9	59 %	58 %	57 %

### V.CONCLUSION

In this study, the surface settlement and vertical pressure at the pipe crown for two cases—with and without geocell

reinforcement—are obtained on the basis of numerical studies (using the finite element method). Comparisons have been made between the finite element models and experimental

works, and good agreement has been obtained. Three different pipe diameters were selected (i.e. 600 mm, 800 mm, and 1000 mm). Three vehicle speeds were chosen (i.e. 20 km/h, 40 km/h, and 60 km/h). The geocell reinforcement was modeled at the sand-subbase interface. The results can be summarized as follows:

1. Geocell reinforcement greatly improves the performance of buried pipes by reducing the vertical pressure above the pipe crown and by reducing the vibration of the pipe.
2. For a pipe diameter of 600 mm under geocell reinforcement, surface settlement decreases by 94 % when the vehicle speed is 20 km/h and by 98 % when the vehicle speed is 60 km/h.
3. For a pipe diameter of 600 mm, using the geocell reinforcement decreases the vertical pressure by 81 % when the vehicle speeds are 20 km/h and 40 km/h, this becomes 82 % when the vehicle speed is 60 km/h. Meanwhile, for a pipe diameter of 800 mm, the percentage decrease to 75% for all vehicle speeds (i.e. 20 km/h, 40 km/h, and 60 km/h). When the pipe diameter is increased to 1000 mm and when geocell reinforcement is used, the values of decrement become 59% when the vehicle speed is 20 km/h, 58% when the vehicle speed is 40 km/h, and 57% when the vehicle speed is 60 km/h.
4. The variance in vehicle speed has no major effect on surface settlement. In addition, pipe diameter has no significant influence on surface settlement.

#### REFERENCES

- [1] Moser, Alma P., and Steven L. Folkman. *Buried Pipe Design*. New York: McGraw-Hill, 2001.
- [2] Rea, Charles, and James K. Mitchell. "Sand reinforcement using paper grid cells." *Symposium on Earth Reinforcement*. ASCE, 1978.
- [3] Tavakoli Mehrjardi, Gh, S. N. Moghaddas Tafreshi, and Andrew Dawson. "Numerical analysis on Buried pipes protected by combination of geocell reinforcement and rubber-soil mixture." *International Journal of Civil Engineering* 13.2 (2015): 90-104.
- [4] Fahem, Hamdy, and Ahmed Mohamed Hassan. "2D PLAXIS finite element modeling of asphalt-concrete pavement reinforced with geogrid." *Journal of Engineering Sciences Assiut University Faculty of Engineering* 42.6 (2014): 1336-1348.
- [5] M. Y. Fattah, "Three-Dimensional Finite Element Simulation of the Buried Pipe Problem in Geogrid Reinforced Soil," vol. 22, no. 5, pp. 60-73, 2016.
- [6] Nirmala, R., and R. Rajkumar. "Finite element analysis of buried UPVC pipe." *Indian Journal of Science and Technology* 9.5 (2016).
- [7] M. Y. Fattah and W. B. M. Redha, "Effect of geocell reinforcement in the mitigation of traffic" *Global Journal of Engineering Science and Research Management*, vol. 3, no. 7, pp. 118-128, 2016.
- [8] Brinkgreve, Ronald BJ, et al. "Beyond the Finite Element Method in Geotechnical Analysis." (2015). 50.
- [9] Zienkiewicz, O. C., and R. L. Taylor. "The Finite Element Method. Solid and Fluid Mechanics. Dynamics and Non-Linearity, Vol. II." (1991): 227-229.
- [10] M. Y. Fattah, W. H. Hassan, and S. E. Rasheed, "Experimental and Numerical Behavior of Flexible Buried Pipes under Geocell Reinforced Subbase Subjected to Repeated Loading," 2017.
- [11] ASTM, D. 2008. D2321 Standard practice for the underground installation of thermoplastic pipe for sewers and other gravity-flow applications. ASTM International, West Conshohocken, PA.
- [12] BSI, B. S. 1980. 5400 Steel, concrete and composite bridges, Part 10: Code of practice for fatigue. British Standards Institution.
- [13] Haas, Ralph, Jamie Walls, and R. G. Carroll. *Geogrid Reinforcement of Granular Bases in Flexible Pavements*. No. 1188. 1988.
- [14] J. Sellmeijer, "Design of geotextile reinforced paved roads and parking

- areas," in *Proceedings of the Fourth International Conference on Geotextiles, Geomembranes and Related Products*, 1990, pp. 177-182.
- [15] T. Kinney, J. Abbott, and J. Schuler, "Benefits of using geogrids for base reinforcement with regard to rutting," *Transportation Research Record: Journal of the Transportation Research Board*, no. 1611, pp. 86-96, 1998.